2023 62nd IEEE Conference on Decision and Control (CDC)
December 13-15, 2023. Marina Bay Sands, Singapore

Estimation of quantum channels using neural networks *

Hailan Ma[1], Zhenhong Sun[1], Shuixin Xiao[2,1,3], Daoyi Dong[2,1], Ian R. Petersen[2]

Abstract— **Quantum process tomography is an essential task for characterizing the dynamics of quantum systems and achieving precise quantum control. In this work, we propose a machine learning-based quantum process tomography method to reconstruct the Choi matrices of quantum channels from the measurements of the output states. Numerical results demonstrate that the proposed method exhibits a significant potential to achieve accurate reconstruction of different quantum channels.**

I. Introduction

The characterization of quantum systems is a fundamental task in quantum control and quantum information processing [1], [2], [3]. The identification of quantum states is indispensable in verifying experimental outcomes, which has been developed as a general scheme, i.e., quantum state tomography. Meanwhile, extraction of the evolution of states (i.e., quantum channels) is another vital task in benchmarking quantum operations and verifying the performance of quantum devices. A typical framework to formulate this issue is known as quantum process tomography (QPT), aiming to specify the parameters of the quantum map from input states to output states.

Based on the system architecture, QPT generally can be classified into three categories: standard quantum process tomography (SQPT), ancilla-assisted process tomography (AAPT), and direct characterization of quantum dynamics (DCDQ) [4]. In SQPT, the input states have the same dimension as the quantum channel, whose parameters are obtained by reconstructing the output states after the evolution. In AAPT and DCQD, an auxiliary system is attached to the system to compose an extended Hilbert space, where the input states are prepared and the measurements are performed [4]. However, due to the technical challenges associated with implementing high-dimensional states in the extended space for AAPT and the requirement of entanglement in DCQD [5], [6], we will focus on SQPT in this paper, where a set of input states evolve into a set of output states and the output states are measured in order to determine the parameters of the quantum channel.

*This work was supported by the Australian Research Council's Future Fellowship funding scheme under Project FT220100656, and U.S. Office of Naval Research Global under Grant N62909-19-1-2129.

[1]School of Engineering and Technology, University of New South Wales, Canberra, ACT 2600, Australia hailanma0413@gmail.com

[2]School of Engineering, The Australian National University, Canberra, ACT 2601, Australia daoyi.dong@anu.edu.au, i.r.petersen@gmail.com

[3]University of Michigan–Shanghai Jiao Tong University Joint Institute, Shanghai Jiao Tong University, Shanghai 200240, China xiaoshuixin@sjtu.edu.cn

Several representations have been proposed for quantum channels, including Kraus operators, the Choi matrix, and the χ matrix [4]. The reconstruction of the Choi matrix of a quantum channel can be achieved through maximum likelihood estimation (MLE), which has been previously studied in [7], [8]. To reconstruct the process matrix of unitary maps, a two-stage QPT method based on linear regression estimation (LRE) has been developed [9], and has been extended to non-unitary operations [10]. Minimum measurement resources required to estimate the completely positive trace-preserving (CPTP) maps have been investigated using direct and convex optimization methods [11], [12]. Additionally, the identification of CPTP maps has been explored using iterative projection algorithms [13], [14].

Quantum process tomography is essentially a data processing problem, where machine learning (ML) techniques [15], [16] can be applied for characterization of patterns from quantum data. The use of ML in various quantum tasks has been extensively investigated [17], [40] and has achieved significant success in applications such as verifying quantum devices [18], controlling quantum systems [19], [20], [21], [22], and compressing quantum data [23], [24]. More recently, the use of ML has been introduced to quantum state tomography and has made remarkable achievements. For instance, fully connected networks [24] and conventional neural networks [25], [26], [27] have been designed to reconstruct both pure and mixed states. The potential of neural networks to denoise state-preparation-and-measurement errors has been investigated [28], and their favorable generalization properties have enhanced the estimation of states under limited resources [29], [30].

For an n-qubit system, there are $(16^n - 4^n)$ real parameters describing a completely positive and trace preserving (CPTP) quantum channel. To estimate a quantum channel under standard QPT, a set of input states are prepared to form a tomographically complete set, spanning the Hilbert subspace, where the minimal number of required input states grows exponentially with n. Similarly, a set of measurement must be performed to reconstruct the output states, with the required measurement resource for each state scaling exponentially with n [31]. In practical applications, the observed distributions may not be well approximated due to limited resources, leading to inaccurate estimation. Since machine learning is capable of extracting information from quantum measurements [25], [26], [27], it is natural to explore how ML can be utilized to characterize quantum channels based on the measurement of the output states.

Drawing inspiration from the success of deep neural networks in reconstructing density matrices of quantum

states, we propose a deep neural network quantum process tomography (DNN-QPT) method to reconstruct the Choi matrix (which has a similar physical interpretation as the density matrix) of a quantum channel. We demonstrate the efficiency and potential of this approach through simulations on different channels, comparing it with traditional methods such as LRE and MLE. Our results show a significant improvement in average fidelity, indicating the potential of DNN-QPT to accurately reconstruct quantum channels. The rest of this paper is organized as follows. Section II introduces several basic concepts about quantum process tomography and traditional methods. In Section III, deep neural network quantum process tomography is presented in detail. Numerical results on different quantum channels are presented in Section IV. Concluding remarks are drawn in Section V.

II. Preliminaries

This section provides an overview of some fundamental concepts related to quantum process tomography. It also provides a brief introduction to traditional methods such as maximum likelihood estimation (MLE) and linear regression estimation (LRE).

A. Representations of quantum channels

Quantum channels can be described as linear maps that transform density matrices into other density matrices. Let Λ be a map that transforms an input state $\rho_{in} \in \mathbb{H}_1$ into an output state $\rho_{out} = \Lambda(\rho_{in}) \in \mathbb{H}_2$. Let d_1 and d_2 be the dimensions of $\mathbb{H}_1$ and $\mathbb{H}_2$, respectively. Generally, d_1 and d_2 are not necessarily equal. In this work, we only consider the case of $d_1 = d_2$ and utilize a unified notation as $d = d_1 = d_2$ to represent the dimension of the quantum channel. However, the notation of d_1 and d_2 are utilized to specify the subsystems that are involved in the Choi matrix representation. For a quantum channel to be considered physical, it must satisfy two conditions: (i) Λ is completely positive (CP), and (i) Λ is trace-preserving (TP). Then, we will introduce different mathematical representations for Λ, including Kraus operators, the Choi matrix and the χ matrix.

Kraus operator representation: The transformation from the input state ρ_{in} to the output state ρ_{out} can be expressed using the Kraus operator-sum representation [32]:

$$\rho_{out} = \Lambda(\rho_{in}) = \sum_i A_i \rho_{in} A_i^\dagger, \tag{1}$$

where A_i is a set of mappings (known as Kraus operators) that maps ρ_{in} to ρ_{out}. This equation already satisfies the condition of complete positivity, and the trace-preserving condition requires the following completeness relation

$$\sum_i A_i^\dagger A_i = \mathbb{I} \tag{2}$$

Choi matrix representation: According to the Choi-Jamiolkowski isomorphism, every quantum channel Λ is in one-to-one correspondence with an operator Q_{Choi} [33], such that

$$\Lambda(\rho_{in}) = \text{Tr}_1(Q_{\text{Choi}}(\rho_{in}^T \otimes \mathbb{I}_{d_2})), \tag{3}$$

where $\text{Tr}_1(\rho)$ denotes the partial trace with respect to the first system, i.e., the reduced state when partially observing the second system [1] and we have

$$Q_{\text{Choi}} = \sum_{ij} |i\rangle\langle j| \otimes \Lambda(|i\rangle\langle j|), \tag{4}$$

indicating that Q_{Choi} characterizes Λ completely [34]. Based on Choi's theorem on completely positive maps, a sufficient condition for Λ to be a CP map is that Q_{Choi} is a positive-semidefinite Hermitian matrix. The condition for Λ to be trace preserving is that the partial trace of Q_{Choi} equals the identity matrix:

$$\text{Tr}_2(Q_{\text{Choi}}) = \mathbb{I}_{d_1}. \tag{5}$$

χ matrix representation: By expanding $\{A_i\}$ in (1) using a fixed set of basis matrices $\{F_i\}$, we can express A_j as $A_i = \sum_j c_{ij} F_j$. Substituting this into (1), we obtain $\Lambda(\rho) = \sum_{jk} F_j \rho F_k^\dagger x_{jk}$, where $x_{jk} = \sum_i c_{ij} c_{ik}^*$. If we define the matrix $C = [c_{ij}]$ and the matrix $X = [x_{ij}]$, then $X = C^T C$, which indicates that X must be Hermitian and positive semidefinite. X is called χ matrix and it is in a one-to-one correspondence with Λ. Hence, we can obtain a full characterization of Λ by reconstructing X [35].

B. Traditional methods

To estimate an unknown quantum process, a series of different input states are input to the process, and positive operator-valued measure (POVM) measurements $\mathbb{P}_k$ are performed on each corresponding output state. Let $\hat{p}_{lm}$ be the observed frequency of the corresponding outcomes from the POVM. The frequency is an experimental approximation of the true probability $p_{lm} = \text{Tr}(\mathbb{P}_l \Lambda(\rho_m))$. The goal of QPT is to determine the parameters of quantum channels using the experimental statistics $\{\hat{p}_{lm}\}$. In particular, we introduce two traditional methods, i.e., maximum-likelihood estimation (MLE) and linear regression estimation (LRE).

MLE is a widely used method for quantum process tomography that aims to maximize the likelihood of the observed data. In particular, we seek to maximize the constrained log-likelihood functional as [8]

$$\arg\max_{Q_{\text{Choi}}} \sum_{lm} \hat{p}_{lm} \ln \text{Tr}\left(Q_{\text{Choi}} \rho_m^T \otimes \mathbb{P}_l\right) - \text{Tr}(K_L \otimes \mathbb{I}_{d_2} Q_{\text{Choi}}), \tag{6}$$

where K_L is a Lagrange multiplier matrix that accounts for the trace-preservation condition in (5). By analyzing the extremal equation, we have

$$K = \sum_{ml} \frac{\hat{p}_{lm}}{\text{Tr}(Q_{\text{Choi}} \rho_m^T \otimes \mathbb{P}_l)} \rho_m^T \otimes \mathbb{P}_l, \tag{7}$$

and $K_L = [\text{Tr}_2(K Q_{\text{Choi}} K)]^{1/2}$. Then we update the estimation as

$$Q_{\text{Choi}} \leftarrow [K_L^{-1} \otimes \mathbb{I}_{d_2}] K Q_{\text{Choi}} K [K_L^{-1} \otimes \mathbb{I}_{d_2}]. \tag{8}$$

Given an admissible guess, e.g., $Q_{\text{Choi}} = \mathbb{I}_{d_1 d_2}/d_2$, one can obtain a solution in an iterative way [7], where the iteration of (7) and (8) continues until the distance between two successive runs is smaller than a given threshold.

LRE is a method that converts a quantum process tomography problem into a parameter estimation problem of a linear regression model [9]. To achieve this, we first introduce a complete basis set of $\mathbb{C}^{d\times d}$, denoted by $\{\sigma_n\}_{i=1}^{d^2}$. For example, the Pauli matrices together with $\mathbb{I}_2$ form a complete basis set of $\mathbb{C}^{2\times 2}$. Then choose a set of linearly independent input states $\{\rho_m\}_{m=1}^{M}$ such that every matrix can be expressed as a finite complex linear combination of σ_n. Through Λ, each input state evolves into an output state, which can be expanded uniquely in the basis set as $\rho_m^{out} = \Lambda(\rho_m) = \sum_{n=1}^{d^2} \theta_{mn}\sigma_n$. Define β_{mn}^{jk} such that $A_j\rho_m A_k^\dagger = \sum_{n=1}^{d^2} \beta_{mn}^{jk}\sigma_n$. From the linear independence of $\{\sigma_n\}$, the reationship between X and α is $\sum_{j,k=1}^{d^2} \beta_{mn}^{jk} X_{jk} = \theta_{mn}$. We define the matrix $\Theta = [\theta_{mn}]$, and arrange the elements β_{mn}^{jk} into an $Md^2 \times d^4$ matrix [35], [10]. Letting vec be the column vectorization function, we obtain a compact equation as

$$B\mathrm{vec}(X) = \mathrm{vec}(\Theta), \tag{9}$$

where B is determined once the bases $\{F_j\}$ and $\{\sigma_n\}$ are chosen. Θ is obtained based on the reconstruction of the output states using experimental data. As such, a least-square solution for the process matrix can be obtained as $\mathrm{vec}(X_{LS}) = (B^T B)^{-1} B^T \mathrm{vec}(\Theta)$ [9]. Considering that X_{LS} might break the positive and trace preserving conditions, a physical projection technique is required to pull it back to a positive matrix [36] and an additional measure is required to guarantee the trace-preserving condition [10].

III. Deep neural network quantum process tomography

In this section, we first introduce the generation of the Choi matrix from the output of neural networks, then propose a machine learning-aided quantum process tomography method, i.e., DNN-QPT, which leverages deep neural networks to reconstruct the Choi matrix of a quantum channel.

A. Choi matrix generation

In SQPT, the expectation values of measurements are linked to a description of the operation like its Choi matrix or χ matrix or Kraus operators. Although they are in principle equivalent, they have different features. The Kraus operator representation is intuitive, as it directly demonstrates the transformation of an input state within a quantum channel in (1). But the Kraus decomposition of a quantum channel is not unique, and there are multiple sets of operators that represent the channel. For example, any two sets of Kraus operators $\{A_k\}$ and $\{B_k\}$ that correspond to the same quantum map can be linked via a unitary matrix U as $B_k = \sum_j U_{kj} A_j$ [1]. The χ matrix together with the basis $\{F_j\}$ completely characterize the map Λ and its value can be simplified when taking a specific basis, e.g., Pauli basis.

The Choi matrix provides a unique and compact representation of a quantum channel and it allows us to compute the output state from the quantum channel following (4). Furthermore, normalizing the Choi matrix to trace 1, we can obtain a physical density matrix as

$$\rho_{\mathrm{Choi}} = \frac{Q_{\mathrm{Choi}}}{\mathrm{Tr}(Q_{\mathrm{Choi}})}, \tag{10}$$

where ρ_{Choi} represents a quantum state obtained from putting half of the maximally entangled state $\frac{1}{d_2}\sum_{ij}|i\rangle\langle j|$ into the map Λ while doing nothing on the other half. For a CPTP map, the partial trace of ρ_{Choi} over $\mathbb{H}_2$ is actually the maximally mixed states $\frac{\mathbb{I}_{d_1}}{d_1}$.

The χ matrix and the Choi matrix are two widely used representations as they both characterize quantum channels precisely. Moreover, they can be easily transformed into each other using basic mathematical computations. In particular, when taking the natural basis in the χ matrix, its value is reduced to Choi matrix. Owing to the physical meaning of the Choi matrix, which is similar to the density matrix used in quantum state tomography, we finally decide on the Choi matrix to represent a quantum channel Λ.

The Choi matrix of a CPTP channel satisfies the following requirements (i) it is a positive semi-definite Hermitian matrix, (ii) its partial trace equals $\mathbb{I}$. To generate a Choi matrix satisfying those conditions, we leverage a lower triangular matrix Q_L to obtain a semi-definite Hermitian matrix as $Q_H = Q_L Q_L^\dagger$. Then, we need to guarantee that it is a physical Choi matrix with trace preserving charateristics (i.e., its partial trace equals to the identity matrix), which can be realized using the following equation

$$Q_1 = [\mathrm{Tr}_2(Q_H)]^{1/2}, \quad Q_{\mathrm{Choi}} = [Q_1^{-1}\otimes\mathbb{I}_{d_2}]Q_H[Q_1^{-1}\otimes\mathbb{I}_{d_2}]. \tag{11}$$

One can check $\mathrm{Tr}_2[Q_{\mathrm{Choi}}] = \mathbb{I}_{d_1}$. Conversely, a lower triangular matrix Q_L that achieves $Q_L Q_L^\dagger = Q_{\mathrm{Choi}}$ can be obtained using the Cholesky decomposition [37]. Notably, a small perturbation term with a small ε can be added to Q_{Choi} with a low rank to avoid convergence issues in the Cholesky decomposition [37].

B. DNN-QPT

Quantum process tomography aims to determine the parameters of a quantum channel that transforms a set of input states into a set of output states. In standard QPT, measurements are performed on the output states to obtain frequencies, which are essential for determining the Choi matrix of the quantum operation. Inspired by the universal approximation theorem [15] which states that any continuous function can be approximated by a multi-layer fully connected neural network, we construct a multi-layer fully connected neural network, to approximate the map function from frequencies to the Choi matrix.

To fully specify a quantum channel, we need to perform measurements on a set of input states that form a tomographically complete set, spanning the Hilbert subspace where the POVM elements are defined. In this work, we consider the input states as the tensor product of single-qubit states as $\left\{\frac{\mathbb{I}}{2}, \frac{\mathbb{I}+\sigma_x}{2}, \frac{\mathbb{I}+\sigma_y}{2}, \frac{\mathbb{I}+\sigma_z}{2}\right\}$. For measurements, we consider the tensor products of Pauli matrices, which are also called the cube measurements [38]. Hence, the obtained frequencies are

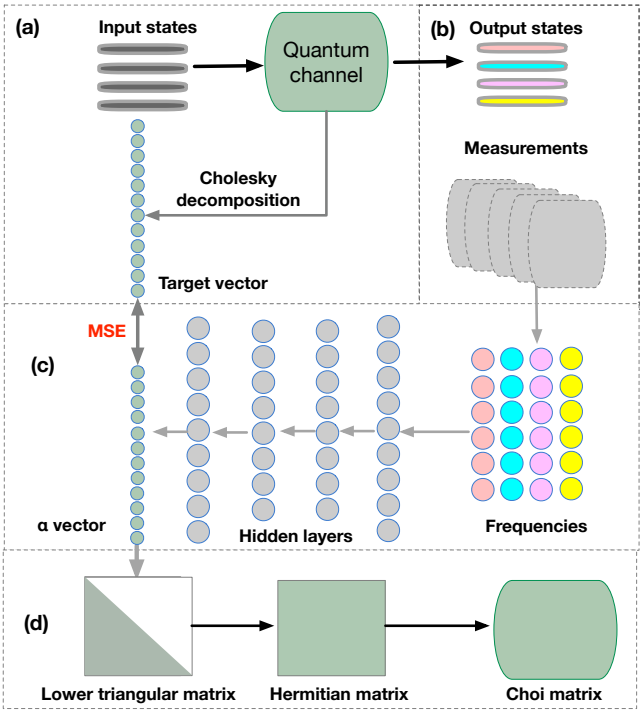

Fig. 1. Schematic of DNN-QPT. (a) Input states are injected into the quantum channel whose Choi matrix is represented as a real vector, (b) Obtain measured statistics by observing the output states, (c) A multi-layer neural network is designed to map the frequencies to the α-vector, (d) Obtain the Choi matrix from the NNs' output.

$4^n \times 6^n$ matrices, where 4^n denotes the number of the input states and 6^n denotes the number of measurement operators. To obtain a $d^2 \times d^2$ Choi matrix from the NNs' output, one may generate a lower triangular matrix Q_L, which can be further split into a real vector with length d^4, called α-vector. This vector can produce a physical Choi matrix after some transformations. Hence, the input layer for DNN-QPT should have 24^n neurons and the output layer should have d^4 neurons. The number of hidden layers and the number of hidden neurons can be adjusted according to the complexity of the problem, e.g., the dimension of the quantum channel.

The QPT procedure using neural networks can be summarized into fours aspects as shown in Fig. 1: (a) A set of input states are injected into the quantum channel, whose Choi matrix can be decomposed into a target vector using the Cholesky decomposition, (b) Measurements are performed on a set of output states, ending up with a set of frequencies, (c) An architecture that utilizes input-hidden-output layers is designed as a parameterized function to map a feature vector comprising of measurement outcomes to an α-vector, (d) The α-vector is finally transformed into a physical Choi matrix. During the training process, the mean square error (MSE) between the constructed α-vector (which is generated from the neural network) and the expected α_{target} vector (which is obtained from the ground truth of a Choi matrix) is taken as the cost function to train the parameters in (c). After the Choi matrix is obtained in (d), the similarity between two quantum channels can be measured as

$$F(Q_1, Q_2) = F_s\left(\frac{Q_1}{\text{Tr}(Q_1)}, \frac{Q_2}{\text{Tr}(Q_2)}\right), \tag{12}$$

where $\frac{Q}{\text{Tr}(Q)}$ denotes the normalized density matrix from the Choi matrix Q and $F_s(\rho_1, \rho_2)$ represents the state fidelity between ρ_1 and ρ_2 [1].

IV. Numerical Results

To test the performance of DNN-QPT, numerical simulations on 1-qubit and 2-qubit quantum channels are carried out. Parameter settings are first presented, and reconstruction of different quantum channels, including unitary channels, Pauli channels, dephasing channels, and depolarizing channels are investigated and compared on different methods.

A. Parameter settings

For each case, 50000 samples are generated by randomly sampling the parameters. We use 97500 samples for training the model of DNN-QPT and 2500 samples for testing the performance of DNN-QPT. For the cube measurements, the 6^n measurements can be grouped into 3^n sets, where each set contains 2^n operators. In practical applications, the measurements are implemented with sets, i.e., each set defines a detector. Hence, we define N as the number of measurement copies in one detector when measuring one input state. Then the number of measurement copies for each input state is $3^n N$, with the total number of measurement copies for all the input states being $12^n N$.

For the deep neural network architecture, 5 hidden layers are utilized, with each hidden layer using 256 neurons for the 1-qubit case and 512 neurons for the 2-qubit case. We utilize the Adam optimizer and a learning rate of 0.0001 to update the parameters of neural networks. $\varepsilon = 10^{-7}$ is utilized to perform the Cholesky decomposition. For the simulations, the Pytorch framework is utilized to construct the deep neural network to run the model. The stopping criterion for MLE is set as the norm difference between two successive runs below 10^{-8}. For LRE, quantum measurements are performed on the output states, with their density matrices reconstructed by a standard quantum state tomography method [9]. In addition, the obtained Choi matrix is transformed into a physical one using some mathematical techniques [10], [36].

B. Unitary channels

A unitary operation on a density matrix can be expressed as a map $\Lambda(\rho) = U\rho U^\dagger$. This map can be represented by a Kraus decomposition with only one Kraus operator. As a result, the Choi matrix only has 1 non-zero eigenvalue. In this work, we generate random unitary matrices using the Haar measure metric that is invariant under group multiplication, which means that any region of $\mathbb{U}_d$ carries the same weight in a group average [39]. Numerical results for different measurement copies are summarized in Fig. 2, where DNN achieves the best log of infidelity. For the 1-qubit case, LRE achieves a little better performance than MLE, while for the 2-qubit case, MLE exhibits a small degree of superiority over

LRE. Based on the above results, the proposed method is effective in estimating unitary channels.

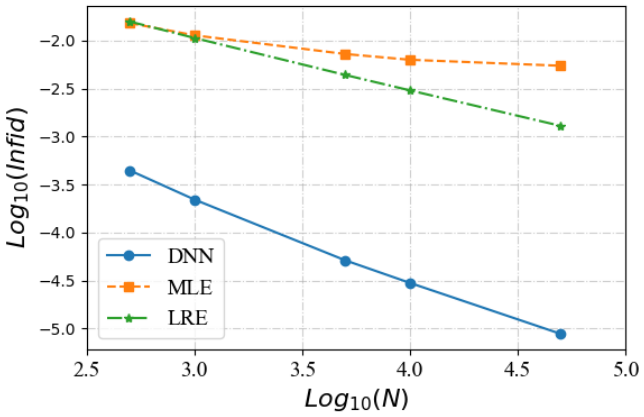

(a) 1-qubit

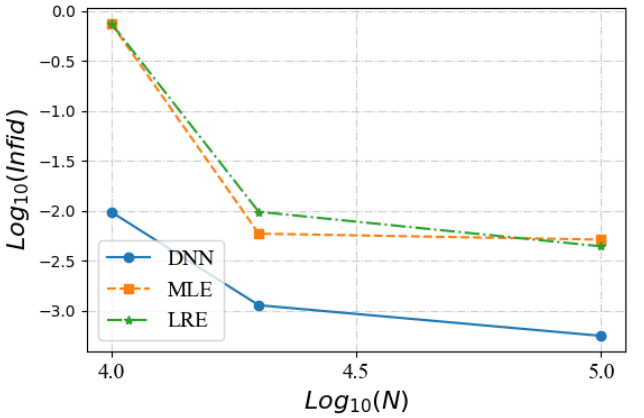

(b) 2-qubit

Fig. 2. The peformance of unitary channels under different measurement copies where Infid denoting infidelity.

C. Error channels

Let $\mathbb{P} = (\mathbb{I}_2, \sigma_x, \sigma_y, \sigma_z)$. Pauli channels are formulated as

$$\Lambda(\rho) = \sum_{P_k \in \mathbb{P}} \omega_k P_k \rho P_k, \tag{13}$$

where $\omega_k \geq 0$ and $\sum_k \omega_k = 1$. Clearly, all of the Kraus operators are Pauli operators, each with its own specific weight ω_k. Dephasing and depolarizing errors are common error channels that can be mathematically described as Pauli channels. In the dephasing channel, the (relative) phase of a qubit flips with a probability ω. For 1-qubit case, the Kraus decomposition includes two operators: $A_1 = \sqrt{1-\omega}\mathbb{I}_2$ and $A_2 = \sqrt{\omega}\sigma_z$. In the depolarizing channel, the Pauli X, Y, Z operators are applied to the state with equal probabilities $\frac{\omega}{3}$, while the state can be fixed with a probability $\sqrt{1-\omega}$. For the 1-qubit case, it can be represented as a Kraus decomposition of four operators:

$$\{A_k\} = \{\sqrt{1-p}\mathbb{I}_2, \sqrt{\frac{\omega}{3}}\sigma_x, \sqrt{\frac{\omega}{3}}\sigma_y, \sqrt{\frac{\omega}{3}}\sigma_z\}. \tag{14}$$

Since $\mathrm{Tr}(\rho) = 1$, the transformation of the state can be written as $\Lambda(\rho) = (1 - \frac{4\omega}{3})\rho + \frac{4\omega}{3}\frac{\mathbb{I}_2}{2}$.

The numerical results for Pauli channels are summarized in Fig. 3, where DNN achieves the best reconstruction accuracy, with MLE and LRE falling behind. The numerical results for dephasing channels and depolarizing channels are summarized in Table I, where the superiority of DNN over LRE and MLE is strong for both dephasing channels and depolaring channels, especially for the 2-qubit case. The large gap between DNN and other traditional methods demonstrates the potential of neural network-aided QPT in reconstructing dephasing and depolarizing channels.

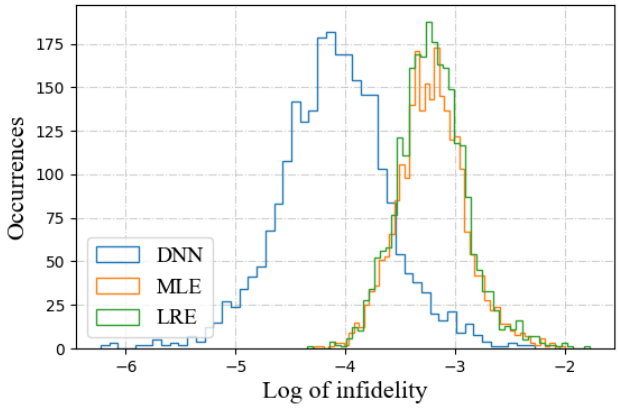

(a) 1-qubit

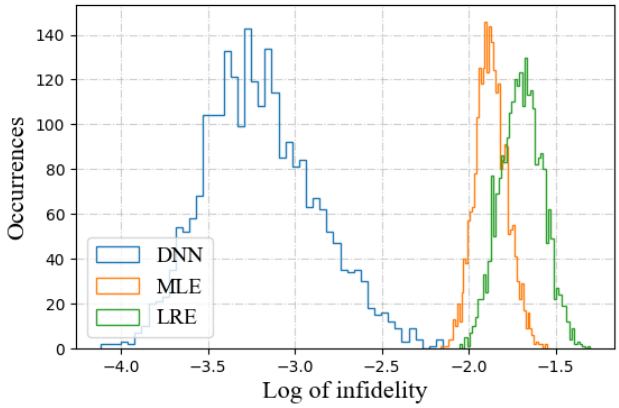

(b) 2-qubit

Fig. 3. The peformance of Pauli channels channels with $N = 10000$.

TABLE I

AVERAGE LOG OF INFIDELITY FOR ERROR CHANNELS WITH $N = 10000$.

Channels / Method	DNN	LRE	MLE
1-qubit dephasing	**1.47e-05**	4.83e-03	5.00e-03
1-qubit depolarizing	**3.30e-05**	1.26e-03	1.08e-03
2-qubit dephasing	**1.30e-06**	2.68e-02	5.00e-03
2-qubit depolarizing	**2.61e-06**	7.33e-03	1.34e-02

V. Conclusion

Quantum process tomography is a central problem in quantum information processing. To leverage the capability of neural networks to capture complex patterns from quantum measured staticstics, we proposed a machine learning adied QPT method to efficiently characterize the Choi matrix of a quantum channel. Simulation results on 1-qubit and 2-qubit quantum channels indicate that the proposed method has the potential to achieve enhanced characterization of different quantum channels, especially for dephasing channels and depolarizing channels. In our future work, we plan to extend the approach to non-trace preserving channels and explore adaptative quantum process tomography using machine learning.

References

[1] M. A. Nielsen and I. L. Chuang, *Quantum Computation and Quantum Information*. Cambridge University Press, 2010.

[2] D. Dong and I. R. Petersen, "Quantum control theory and applications: a survey," *IET Control Theory & Applications*, vol. 4, no. 12, pp. 2651–2671, 2010.

[3] D. Dong, and I. R. Petersen, *Learning and Robust Control in Quantum Technology*. Springer Nature SwitzerlandAG, 2023.

[4] M. Mohseni, A. T. Rezakhani, and D. A. Lidar, "Quantum-process tomography: Resource analysis of different strategies," *Physical Review A*, vol. 77, no. 3, p. 032322, 2008.

[5] D. Dong and I. R. Petersen, "Quantum estimation, control and learning: Opportunities and challenges," *Annual Reviews in Control*, vol. 54, pp. 243-251, 2022.

[6] L.-B. Fan, C.-C. Shu, D. Dong, J. He, N. E. Henriksen, and F. Nori, "Quantum coherent control of a single molecular-polariton rotation," *Physical Review Letters*, vol. 130, no. 4, p. 043604, 2023.

[7] J. Řeháček, Z. Hradil, and M. Ježek, "Iterative algorithm for reconstruction of entangled states," *Physical Review A*, vol. 63, no. 4, p. 040303, 2001.

[8] M. Ježek, J. Fiurášek, and Z. Hradil, "Quantum inference of states and processes," *Physical Review A*, vol. 68, no. 1, p. 012305, 2003.

[9] B. Qi, Z. Hou, L. Li, D. Dong, G.-Y. Xiang, and G.-C. Guo, "Quantum state tomography via linear regression estimation," *Scientific Reports*, vol. 3, p. 3496, 2013.

[10] S. Xiao, Y. Wang, D. Dong, and J. Zhang, "Two-stage solution of quantum process tomography in the natural basis," in *2022 IEEE 61st Conference on Decision and Control (CDC)*, pp. 5807–5812, IEEE, 2022.

[11] M. Zorzi, F. Ticozzi, and A. Ferrante, "Estimation of quantum channels: Identifiability and ml methods," in *2012 IEEE 51st IEEE Conference on Decision and Control (CDC)*, pp. 1674–1679, IEEE, 2012.

[12] M. Zorzi, F. Ticozzi, and A. Ferrante, "Minimal resources identifiability and estimation of quantum channels," *Quantum Information Processing*, vol. 13, pp. 683–707, 2014.

[13] G. C. Knee, E. Bolduc, J. Leach, and E. M. Gauger, "Quantum process tomography via completely positive and trace-preserving projection," *Physical Review A*, vol. 98, no. 6, p. 062336, 2018.

[14] T. Surawy-Stepney, J. Kahn, R. Kueng, and M. Guta, "Projected least-squares quantum process tomography," *Quantum*, vol. 6, p. 844, 2022.

[15] Y. LeCun, Y. Bengio, and G. Hinton, "Deep learning," *Nature*, vol. 521, no. 7553, pp. 436–444, 2015.

[16] I. Goodfellow, Y. Bengio, and A. Courville, *Deep Learning*. MIT Press, 2016.

[17] J. Biamonte, P. Wittek, N. Pancotti, P. Rebentrost, N. Wiebe, and S. Lloyd, "Quantum machine learning," *Nature*, vol. 549, no. 7671, p. 195, 2017.

[18] D. Lennon, H. Moon, L. Camenzind, L. Yu, D. Zumbühl, G. Briggs, M. Osborne, E. Laird, and N. Ares, "Efficiently measuring a quantum device using machine learning," *npj Quantum Information*, vol. 5, no. 1, pp. 1–8, 2019.

[19] C. Chen, D. Dong, H.-X. Li, J. Chu, and T.-J. Tarn, "Fidelity-based probabilistic Q-learning for control of quantum systems," *IEEE Transactions on Neural Networks and Learning Systems*, vol. 25, no. 5, pp. 920–933, 2013.

[20] H. Ma, D. Dong, S. X. Ding, and C. Chen, "Curriculum-based deep reinforcement learning for quantum control," *IEEE Transactions on Neural Networks and Learning Systems*, 2022.

[21] D. Dong, X. Xing, H. Ma, C. Chen, Z. Liu, and H. Rabitz, "Learning-based quantum robust control: algorithm, applications, and experiments," *IEEE Transactions on Cybernetics*, vol. 50, no. 8, pp. 3581–3593, 2020.

[22] R.-B. Wu, H. Ding, D. Dong, and X. Wang, "Learning robust and high-precision quantum controls," *Physical Review A*, vol. 99, no. 4, p. 042327, 2019.

[23] C.-J. Huang, H. Ma, Q. Yin, J.-F. Tang, D. Dong, C. Chen, G.-Y. Xiang, C.-F. Li, and G.-C. Guo, "Realization of a quantum autoencoder for lossless compression of quantum data," *Physical Review A*, vol. 102, no. 3, p. 032412, 2020.

[24] H. Ma, C.-J. Huang, C. Chen, D. Dong, Y. Wang, R.-B. Wu, and G.-Y. Xiang, "On compression rate of quantum autoencoders: Control design, numerical and experimental realization," *Automatica*, vol. 147, p. 110659, 2023.

[25] S. Lohani, B. Kirby, M. Brodsky, O. Danaci, and R. T. Glasser, "Machine learning assisted quantum state estimation," *Machine Learning: Science and Technology*, vol. 1, no. 3, p. 035007, 2020.

[26] O. Danaci, S. Lohani, B. T. Kirby, and R. T. Glasser, "Machine learning pipeline for quantum state estimation with incomplete measurements," *Machine Learning: Science and Technology*, vol. 2, no. 3, p. 035014, 2021.

[27] S. Lohani, T. A. Searles, B. T. Kirby, and R. T. Glasser, "On the experimental feasibility of quantum state reconstruction via machine learning," *IEEE Transactions on Quantum Engineering*, vol. 2, pp. 1–10, 2021.

[28] A. M. Palmieri, E. Kovlakov, F. Bianchi, D. Yudin, S. Straupe, J. D. Biamonte, and S. Kulik, "Experimental neural network enhanced quantum tomography," *npj Quantum Information*, vol. 6, no. 1, pp. 1–5, 2020.

[29] H. Ma, D. Dong, and I. R. Petersen, "On how neural networks enhance quantum state tomography with limited resources," in *2021 60th IEEE Conference on Decision and Control (CDC)*, pp. 4146–4151, IEEE, 2021.

[30] H. Ma, D. Dong, I. R. Petersen, C.-J. Huang, and G.-Y. Xiang, "On how neural networks enhance quantum state tomography with constrained measurements," *arXiv preprint arXiv:2111.09504*, 2023.

[31] Z. Hou, H.-S. Zhong, Y. Tian, D. Dong, B. Qi, L. Li, Y. Wang, F. Nori, G.-Y. Xiang, C.-F. Li, *et al.*, "Full reconstruction of a 14-qubit state within four hours," *New Journal of Physics*, vol. 18, no. 8, p. 083036, 2016.

[32] K.-E. Hellwig and K. Kraus, "Pure operations and measurements," *Communications in Mathematical Physics*, vol. 11, no. 3, pp. 214–220, 1969.

[33] M.-D. Choi, "Completely positive linear maps on complex matrices," *Linear algebra and its applications*, vol. 10, no. 3, pp. 285–290, 1975.

[34] M. Jiang, S. Luo, and S. Fu, "Channel-state duality," *Physical Review A*, vol. 87, no. 2, p. 022310, 2013.

[35] Y. Wang, D. Dong, B. Qi, J. Zhang, I. R. Petersen, and H. Yonezawa, "A quantum Hamiltonian identification algorithm: Computational complexity and error analysis," *IEEE Transactions on Automatic Control*, vol. 63, no. 5, pp. 1388–1403, 2017.

[36] J. A. Smolin, J. M. Gambetta, and G. Smith, "Efficient method for computing the maximum-likelihood quantum state from measurements with additive Gaussian noise," *Physical Review Letters*, vol. 108, no. 7, p. 070502, 2012.

[37] N. J. Higham, *Analysis of the Cholesky decomposition of a semi-definite matrix*. Oxford University Press, 1990.

[38] M. D. De Burgh, N. K. Langford, A. C. Doherty, and A. Gilchrist, "Choice of measurement sets in qubit tomography," *Physical Review A*, vol. 78, no. 5, p. 052122, 2008.

[39] F. Mezzadri, "How to generate random matrices from the classical compact groups," *arXiv preprint math-ph/0609050*, 2006.

[40] H. Ma, S. Xiao, D Dong, I. Petersen, "Tomography of quantum detectors using neural networks", *22th World Congress of the International Federation of Automatic Control (IFAC),* Yokohama, Japan, 9 July-14 July, 2023.